

SUPPLEMENTARY INFORMATION

Spatially resolved ultrafast magnetic dynamics launched at a complex oxide hetero-interface

M. Först^{1,2*}, A.D. Caviglia^{3*}, R. Scherwitzl⁴, R. Mankowsky^{1,2}, P. Zubko⁴,
V. Khanna^{1,5,6}, H. Bromberger^{1,2}, S.B. Wilkins⁷, Y.-D. Chuang⁸, W.S. Lee⁹, W.F.
Schlotter¹⁰, J.J. Turner¹⁰, G.L. Dakovski¹⁰, M.P. Minitti¹⁰, J. Robinson¹⁰, S.R.
Clark^{5,11}, D. Jaksch^{5,11}, J.-M. Triscone⁴, J.P. Hill⁷, S.S. Dhesi⁶, and A. Cavalleri^{1,2,5}

¹*Max Planck Institute for the Structure and Dynamics of Matter, 22761 Hamburg, Germany*

²*Center for Free Electron Laser Science, 22761 Hamburg, Germany*

³*Kavli Institute of Nanoscience, Delft University of Technology, 2628 CJ Delft, The Netherlands*

⁴*Department of Quantum Matter Physics, Université de Genève, 1211 Genève, Switzerland*

⁵*Department of Physics, Clarendon Laboratory, University of Oxford, Oxford OX1 3PU, UK*

⁶*Diamond Light Source, Didcot, Oxfordshire OX11 0QX, UK*

⁷*Condensed Matter Physics and Materials Science Department, Brookhaven National Laboratory, Upton 11973, New York, USA*

⁸*Advanced Light Source, Lawrence Berkeley Laboratory, Berkeley 94720, California, USA*

⁹*The Stanford Institute for Materials and Energy Sciences (SIMES), Stanford Linear Accelerator Center (SLAC) National Accelerator Laboratory and Stanford University, Menlo Park 94025, California, USA*

¹⁰*Linac Coherent Light Source, Stanford Linear Accelerator Center (SLAC) National Accelerator Laboratory, Menlo Park 94025, California, USA*

¹¹*Centre for Quantum Technologies, National University of Singapore, Singapore 117543, Singapore*

*These authors contributed equally to this work.

S1. Boundary induced melting of magnetic order

Capturing the connections between spin and charge dynamics in nickelates invariably requires a multi-band d - p orbital Hubbard-like model, in which full degeneracy of the Ni $3d$ orbitals and the oxygen $2p$ orbitals, as well as their hybridization, is taken into account^{1,2}. While the precise mechanistic description of the vibrational excitation involves such material specific calculations, here as a first step, we explore the generic effects of boundary excitations in a simpler model Hamiltonian.

Model Hamiltonian

To qualitatively describe the dynamics of the nickelate thin film we consider a single-band Hubbard model-like Hamiltonian³ of the form

$$\hat{H} = -t \sum_{\langle i,j \rangle} (\hat{c}_{i\sigma}^\dagger \hat{c}_{j\sigma} + h.c.) + U \sum_j \hat{n}_{j\uparrow} \hat{n}_{j\downarrow} + J_{zz} \sum_{\langle i,j \rangle} \hat{s}_i^z \hat{s}_j^z$$

where $\hat{c}_{i\sigma}^\dagger$ is the creation operator for an electron of spin σ on site i , $\hat{n}_{i\sigma}$ is the corresponding number operator and $\hat{s}_i^z = \frac{1}{2}(\hat{n}_{i\uparrow} - \hat{n}_{i\downarrow})$ is the spin projection along the z axis (out-of-plane direction). We denote nearest-neighbor sites in the lattice as $\langle i,j \rangle$, t as the hopping amplitude, U as the on-site Coulomb repulsion, and J_{zz} as an additional Ising spin interaction strength. At half-filling, and in the strong-coupling limit $U/t \gg 1$, the dynamics of the spin sector arising from \hat{H} is an XXZ model

$$\hat{H}_{XXZ} = J \sum_{\langle i,j \rangle} (\hat{s}_i^x \hat{s}_j^x + \hat{s}_i^y \hat{s}_j^y + \Delta \hat{s}_i^z \hat{s}_j^z),$$

where $J = 4t^2/U$ and $\Delta = 1 + J_{zz}/J$. Since the nickelate film displays antiferromagnetic ordering with a well defined orientation we have included the Ising interaction $J_{zz} > 0$ which breaks the rotational invariance of the $\Delta = 1$ isotropic Heisenberg model. For $J_{zz}/J \gg 1$ the ground state of the XXZ model

has classical Ising character akin to a simple Neel state $\uparrow\uparrow \cdots \downarrow\downarrow$ modified by in-plane spin-flip fluctuations.

Within this model framework we now investigate how magnetic and electronic dynamics nucleated at the boundary of the film can propagate through the system, and the effects their motion has on the magnetic ordering.

Magnetic dynamics

One possibility is that an interfacial quench of the film generates localized spin-flips of the antiferromagnetic order, which subsequently evolve according to the XXZ Hamiltonian \hat{H}_{XXZ} . After performing a Holstein-Primakoff transformation⁴ and retaining only the lowest order terms an antiferromagnetic spin-wave (magnon) dispersion relation is obtained as⁵

$$\epsilon(\vec{q}) = \eta \frac{J}{2} \sqrt{\Delta^2 - \gamma(\vec{q})},$$

where \vec{q} is the quasi-momentum in a bipartite lattice with coordination number η and $\gamma(\vec{q}) = \frac{1}{\eta} \sum_{\vec{a}} e^{i \vec{q} \cdot \vec{a}}$ with \vec{a} being the real space vectors connecting one site to all its nearest neighbors. In 3D simple cubic lattice with spacing a we have that $\gamma(\vec{q}) = \frac{1}{3} [\cos(q_x a) + \cos(q_y a) + \cos(q_z a)]$.

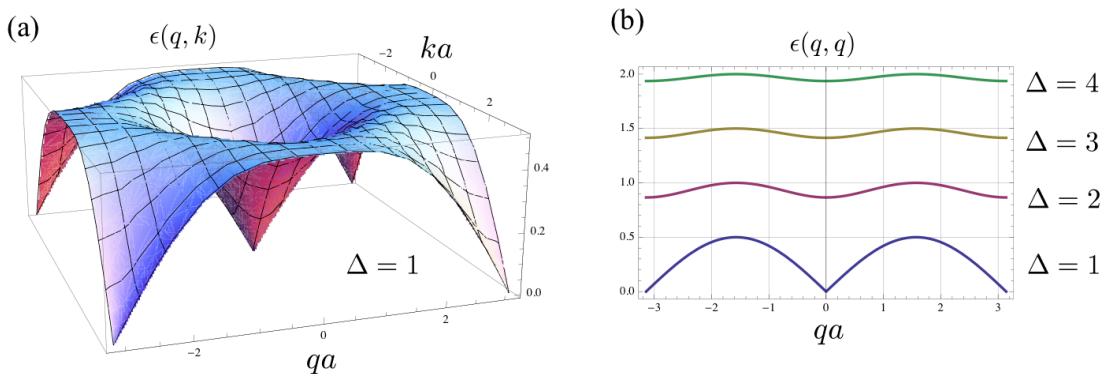


Fig. S1: (a) The antiferromagnetic spin-wave dispersion relation $\epsilon(q, k)$ for the XXZ spin model in a 2D square lattice at the isotropic Heisenberg limit $\Delta = 1$. (b) Diagonal cuts through of the dispersion relation $\epsilon(q, q)$ for different values of $\Delta \geq 1$.

In Fig. S1(a), the dispersion $\epsilon(q, k)$ for a 2D square lattice is shown for $\Delta = 1$ and presents a gapless mode $\vec{q} = (0,0)$ around which the spectrum is linear $\epsilon(\vec{q}) \sim |\vec{q}|$. An additional zero mode is present at the Brillouin zone edge $\vec{q} = (\pi, \pi)$, corresponding to the antiferromagnetic ordering wave-vector, as direct result of having broken the continuous rotational symmetry. However, the more relevant situation for the nickelate film is when an anisotropy $\Delta > 1$ is present. As can be seen in Fig. S1(b), an increasing Δ quickly introduces a gap at all quasi-momentum \vec{q} and flattens $\epsilon(\vec{q})$ leading to a suppression of the spin-wave group velocity. This reflects the detuning of spin-flip transitions with amplitude $J < J_{zz}$ which control the motion.

As a result the propagation of localized magnon packet in real space, corresponding to coherent superposition of all spin-wave momenta, will be substantially reduced by the anisotropy. Thus, magnetic dynamics nucleated at the boundary will remain localized there. This is readily confirmed by time-dependent mean-field calculations. Further to this lack of propagation, for strong anisotropies, the XXZ model is also known to possess highly excited edge-locked bound states which pin ferromagnetic regions to open boundaries⁶.

The purely magnetic process of melting the bulk antiferromagnetic order by boundary excitations is also not favored energetically. Magnons possess an energy governed by, and therefore the same order as, the interaction which stabilizes the order. Assuming that the total excitation energy of the boundary magnons scales with the interfacial area, this will never be energetically sufficient to cause the complete melting of the antiferromagnetic order in a fraction of the bulk.

Charge dynamics

We now consider the consequences of the substrate vibration nucleating charge-neutral holon (vacancy $|0\rangle$) and doublon (double occupancy $|\uparrow\downarrow\rangle$) pairs at the boundary of the film. Compared with a “magnetic only” picture, this scenario, where itinerant charge carriers are generated, is also consistent with the concomitant insulator-metal transition observed in the THz probe experiment.

To describe the dynamics of the system when doped with charge carriers requires the full Hubbard Hamiltonian \hat{H} which now involves two new energy scales U and t not previously exposed in \hat{H}_{XXZ} . Once U is sufficiently large then regime $t > J_{zz} > 4t^2/U$ is attained where the anisotropy still dominates the magnetic interactions while hopping exceeds all magnetic energy scales. Since the kinetic energy of localized holon-doublon pairs is $\sim t$ this indicates that, in contrast to magnons, charge carriers can be energetic enough to both propagate and significantly excite the magnetic sector.

The motion of holons or doublons in an antiferromagnet can scramble the antiferromagnetic order creating a paramagnet. At $T = 0$, this is a long-studied problem^{7,8,9,10}. Key insight is that the motion of charge carriers is greatly impeded by the presence of antiferromagnetic order. Approximations, such as Brinkman and Rice’s retraceable path approach⁷, indicate the motion of charge carriers is akin to Brownian motion even at $T = 0$. Moreover, due to the ‘string’ magnetic excitations, which trail behind the trajectory of a charge in an antiferromagnet, it is expected that their propagation will be confined to a finite region to account for the loss of kinetic energy to the magnetic sector^{9,10}.

We introduce an approximate classical stochastic model to capture these effects based on a Pauli master equation¹¹

$$\frac{d}{d\tau}P_j(\tau) = \sum_{k \neq j} W(k \rightarrow j)P_k(\tau) - \sum_{k \neq j} W(j \rightarrow k)P_j(\tau),$$

describing the evolution in time τ of probability $P_j(\tau)$ of occupying a particular configuration j of spins and charges in the Hubbard lattice, e.g. $|j\rangle = |\uparrow\downarrow\uparrow\downarrow\uparrow\downarrow\cdots\rangle$. The transition rate $W(k \rightarrow j)$ from configuration k to j is then defined as

$$W(k \rightarrow j) = \begin{cases} w, & E_j - E_{\text{init}} \leq \mathcal{E} \\ 0, & \text{otherwise} \end{cases},$$

where w is a constant rate, E_j is the energy of configuration j and E_{init} is the energy for the initial boundary excited configuration evaluated with the Hubbard model when hopping $t = 0$, and \mathcal{E} is the total excitation energy. Carriers therefore diffuse through the lattice at a fixed rate w until the energy deposited into system by moving to a new configuration exceeds \mathcal{E} , at which point the rate abruptly drops to zero. This simple choice enforces a form of energy conservation which limits the capacity of the holons and doublons to excite the magnetic sector.

The resulting stochastic evolution starting from an antiferromagnetic configuration with holon-doublon pairs randomly distributed along the boundary was simulated using dynamical Monte Carlo¹². A 40×40 2D square lattice was used with periodic boundaries along the interface x direction and open boundaries in the film z direction. In Fig. S2(a), we report the staggered magnetization averaged over the x direction as a function of the d_z distance into the film and time. Specific time slices are also displayed in Fig. S2(b). Together, these show that initially there is fast evolution of an error-function diffusion front dictated by the rate w which strongly demagnetizes the lattice behind it. The specific parameters \mathcal{E} and w used (see figure caption) were chosen to best

match the features seen in the experimental data. Consequently after ~ 3 ps the diffusion front abruptly stalls, due to the energy limit \mathcal{E} , corresponding to when antiferromagnetic order has been melted in approximately half the film. This emergence of a gradual boundary between paramagnetic and antiferromagnetic regions in the film is further highlighted by the dynamical suppression of the $qa = \pi$ peak in the static structure factor

$$F(q) = \sum_{jl} e^{iq(j-l)a} \langle \hat{s}_j^z \hat{s}_l^z \rangle,$$

shown in Fig. S2(c) as a function of time.

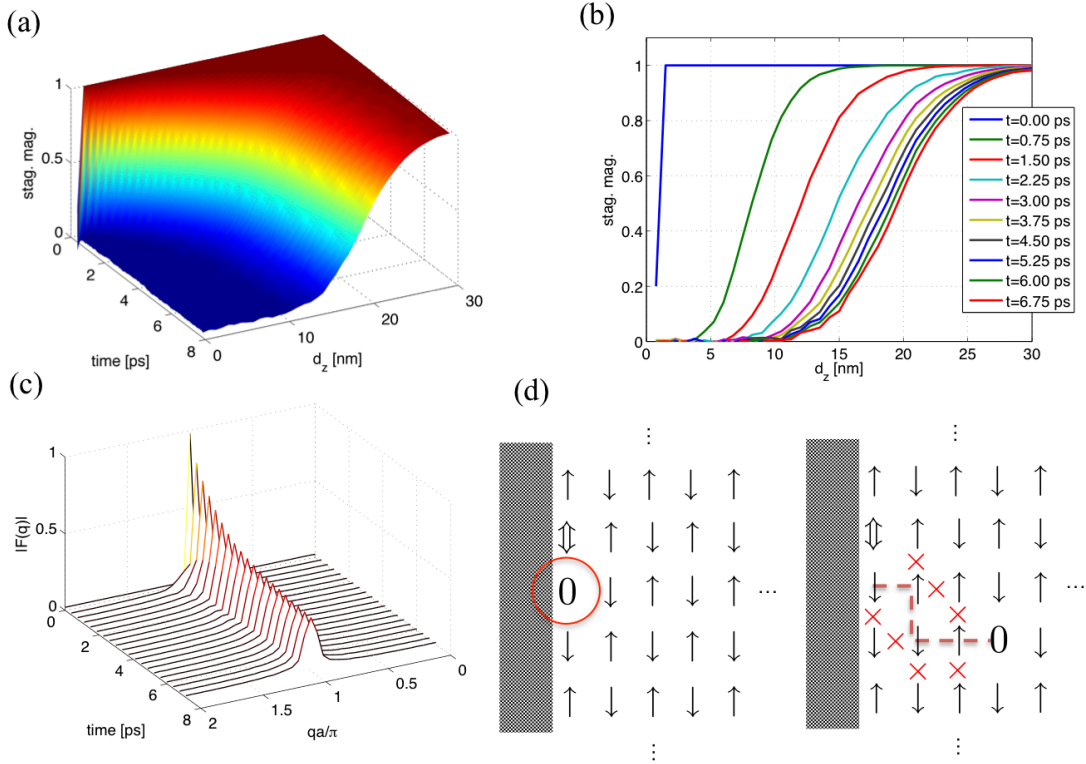


Fig. S2 (a) The staggered magnetization for a 2D square lattice as a function of distance from the interface (film depth) and time averaged over the transverse direction. (b) Slices of plot (a) for given times. (c) The magnetic structure factor $F(q)$, for the lattice as function of time. To produce results quantitatively resembling the experimental data these calculations used a total of 32 holon-doublon pairs initiated with an excitation energy \mathcal{E} equivalent to $\sim 47J_{zz}$ per charge carrier and a diffusion time constant $w^{-1} \sim 38$ fs. (d) An illustration of how the stochastic motion of a charge carrier from the boundary (hole in this case) scrambles the antiferromagnetic order of the system. The dotted line denotes its trajectory and the \times 's mark the magnetic interactions which are now ferromagnetic bonds.

While this model has ad-hoc features it nonetheless illustrates that diffusive motion of charge carriers is highly effective at scrambling antiferromagnetic order simply by the shuffling of spins along a trajectory as shown in Fig. S2(d). The further inclusion of an energy cut-off \mathcal{E} however was essential to capture the localization effects^{9,10} caused by the loss of kinetic energy of the charge carriers as they excite the magnetic degrees of freedom, also shown in Fig. S2(d). Both these effects appear to be qualitatively present in the experimental results.

S2. In-plane magnetization dynamics following mid-IR excitation

Here, we present the mid-IR induced dynamics of the antiferromagnetic in-plane correlations. Figure S3 shows the transverse rocking curves (theta scans) measured at three early time delays across the phase transition. The experimental conditions are identical to those presented in the main paper. Fitting Gaussian functions to these data sets yields FWHM values of 0.65 ± 0.1 degrees (at -0.5 ps), 0.66 ± 0.1 degrees (at $+1.5$ ps) and 0.63 ± 0.1 degrees (at $+3$ ps). Thus, we conclude the in-plane correlation length remains unchanged. This effect results from the pump spot size being far larger than the magnetic domain size along this direction.

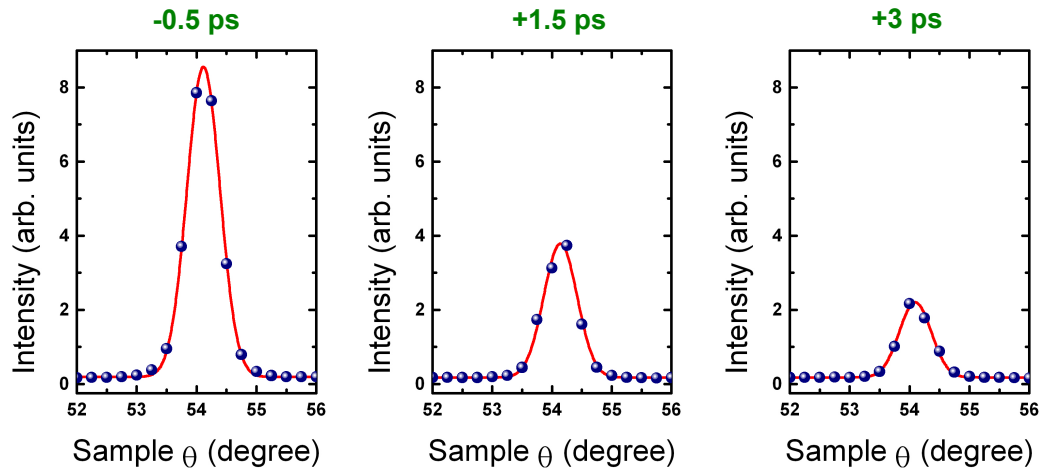


Fig. S3 Rocking curves of the $(1/4 \ 1/4 \ 1/4)$ diffraction peak at selected, early time delays before and after the mid-infrared excitation. The widths of these peaks represent the in-plane correlation length. Note, at 3 ps time delay, the system has undergone the demagnetization process along the out-of-plane direction, before it starts recovering.

References (Supplementary Information)

1. Mizokawa, T., Khomskii, D.I. & Sawatzky, G.A. Spin and charge ordering in self-doped Mott insulators. *Phys. Rev. B* **61**, 11263-11266 (2000).
2. Lee, S. Chen, R. & Balents, L. Landau theory of charge and spin ordering in the nickelates. *Phys. Rev. Lett.* **106**, 016405 (2011).
3. Hubbard, J. Electron Correlations in Narrow Energy Bands. *Proc. Roy. Soc. (London) A* **276**, 238-257 (1963).
4. Holstein T. & Primakoff, H. Field dependence of the intrinsic domain magnetization of a ferromagnet. *Phys. Rev.* **58**, 1098-1113 (1940).
5. Mattis, D.C. *The theory of magnetism made simple* (World Scientific, Singapore, 2006).
6. Haque M. Self-similar spectral structures and edge-locking hierarchy in open-boundary spin chains. *Phys. Rev. A* **82**, 012108 (2010).
7. Brinkman W.F. & Rice T.M. Single-particle excitations in magnetic insulators. *Phys. Rev. B* **2**, 1324-1338 (1970).
8. Kane C.L., Lee P.A. & Read, N. Motion of a single hole in a quantum antiferromagnet. *Phys. Rev. B* **39**, 6880-6897 (1989).
9. Buleavskii, L.N., Nagaev E.L. & Khomskii, D.I. A new type of auto-localized state of a conduction electron in an antiferromagnetic semiconductor. *Sov. Phys. - JETP* **27**, 836-838 (1968).
10. Khomskii, D.I. *Basic aspects of the quantum theory of solids* (Cambridge University Press, Cambridge, 2010).
11. Zwanzig, R. *Nonequilibrium Statistical Mechanics* (Oxford University Press, Oxford, 2001).

12. Jansen, A.P.J. An introduction to Monte Carlo simulations of surface reactions.
arXiv:cond-mat/0303028 (2003).